Article

Cell Host & Microbe

Crosstalk between three CRISPR-Cas types enables primed type VI-A adaptation in *Listeria seeligeri*

Graphical abstract

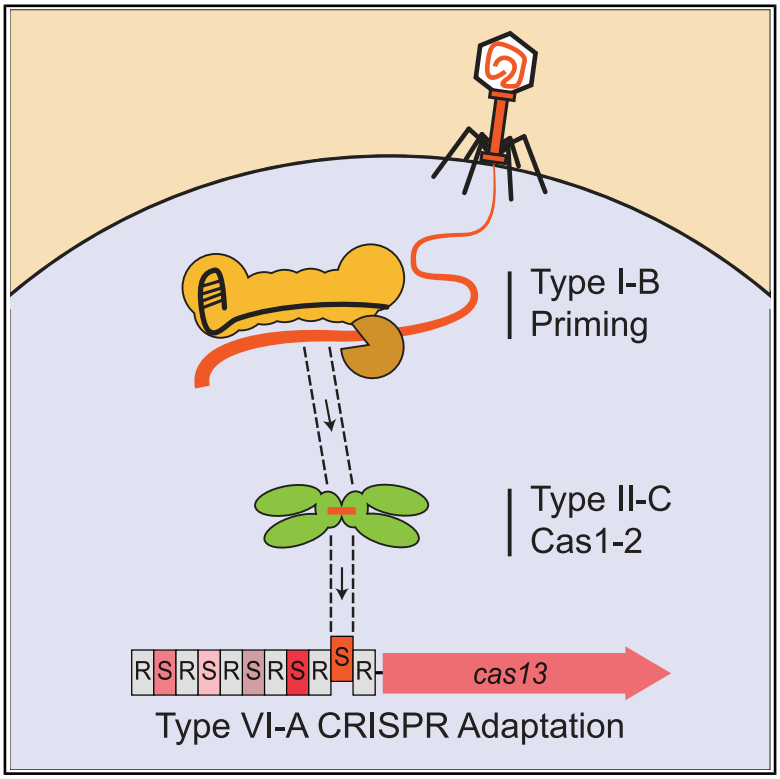

Authors

Shally R. Margolis,
Alexander J. Meeske

Correspondence

meeske@uw.edu

In brief

Margolis et al. describe a mechanism by which the RNA-targeting CRISPR-Cas13 system acquires new immunological memories in its native host *Listeria seeligeri*. The system relies on the machinery of two co-occurring CRISPR types, which work together to acquire DNA fragments from invading phages.

Highlights

- *Listeria* type VI-A CRISPR can acquire spacers using a type II-C Cas1-2 integrase
- Type II-C Cas1-2 exhibits promiscuous spacer integration activity
- Type I-B cross-primes type VI-A spacer acquisition via type II-C Cas1-2
- Type VI systems frequently share targets with co-occurring CRISPR types

Margolis & Meeske, 2025, Cell Host & Microbe *33*, 1–11
September 10, 2025
https://doi.org/10.1016/j.chom.2025.05.020

CellPress

Please cite this article in press as: Margolis and Meeske, Crosstalk between three CRISPR-Cas types enables primed type VI-A adaptation in *Listeria seeligeri*, Cell Host & Microbe (2025), https://doi.org/10.1016/j.chom.2025.05.020

Cell Host & Microbe

CellPress

Article

Crosstalk between three CRISPR-Cas types enables primed type VI-A adaptation in *Listeria seeligeri*

Shally R. Margolis[1] and Alexander J. Meeske[1,2,*]
[1]Department of Microbiology, University of Washington, Seattle, WA 98109, USA
[2]Lead contact
*Correspondence: meeske@uw.edu
https://doi.org/10.1016/j.chom.2025.05.020

SUMMARY

CRISPR-Cas systems confer adaptive immunity to their prokaryotic hosts through the process of adaptation, where sequences are captured from foreign nucleic acids and integrated as spacers in the CRISPR array, thereby enabling crRNA-guided interference against new threats. While the Cas1-2 integrase is critical for adaptation, it is absent from many CRISPR-Cas loci, rendering the mechanism of spacer acquisition unclear for these systems. In this study, we show that the RNA-targeting type VI-A CRISPR system of *Listeria seeligeri* acquires spacers from DNA substrates through the action of a promiscuous Cas1-2 integrase encoded by a co-occurring type II-C system, in a transcription-independent manner. We further demonstrate that the type II-C integration complex is strongly stimulated by preexisting spacers in a third CRISPR system (type I-B), which imperfectly match phage targets and prime type VI-A adaptation. Altogether, our results reveal an unprecedented degree of communication among CRISPR-Cas loci encoded by a single organism.

INTRODUCTION

Clustered regularly interspaced short palindromic repeats (CRISPR) loci and associated (Cas) proteins are widespread prokaryotic adaptive immune systems that engage in RNA-guided surveillance and cleavage of foreign nucleic acids.[1–5] CRISPR loci are composed of short (~30 bp) repetitive DNA elements with equally short "spacer" segments of foreign origin inserted between them. Naive CRISPR immunity occurs in two phases. The first phase is adaptation, in which spacer sequences are captured from invading foreign genetic elements such as bacteriophages or plasmids, and are inserted into the CRISPR locus to immunize the host against infection.[1,6] The second phase is interference, in which the CRISPR locus is transcribed and processed into small crRNAs, which associate with Cas nucleases to perform sequence-specific nucleic acid recognition and cleavage, ultimately neutralizing invading elements that match spacer sequences.[2–5] Two decades of bioinformatic mining have uncovered millions of unique CRISPR loci, categorized into 6 broad types and 35 subtypes, with highly diverse gene content and function.[7–9]

Crucial to the adaptive nature of CRISPR immunity is the ability to acquire new spacers and thus gain heritable memory that protects the host from future infection. In all experimentally characterized CRISPR systems, spacer acquisition requires Cas1 and Cas2, which form a Cas1-2 integrase complex that captures sequences from free DNA ends and inserts new spacer-repeat units into the CRISPR array, resulting in its expansion.[10–13] Phages readily escape CRISPR immunity by evolving mutations in the targeted genomic region that prevent recognition and/or cleavage by Cas nucleases.[14] To rapidly reestablish immunity against a changing viral population, many CRISPR systems have evolved mechanisms for "primed" adaptation. During this process, interference machinery equipped with crRNAs that imperfectly match a phage genome fails to directly neutralize the target but strongly stimulates the acquisition of new spacers from target-proximal regions of DNA.[15–17] Priming has been best characterized in type I CRISPR systems, in which the Cascade surveillance complex bound to a mismatched target recruits the Cas1-2 integrase, which in turn recruits the helicase-nuclease Cas3.[18] The Cas1-2-3 complex then translocates along DNA emanating from the target, processing new spacers for immunization.[18–20] Primed adaptation has also been observed for type II CRISPR systems, which require the nuclease activity of Cas9 to generate free DNA ends that serve as substrates for further spacer acquisition.[21]

Many CRISPR-Cas systems do not encode Cas1-2, leading to the question of whether and how these systems are able to acquire new spacers.[8] Such systems are thought to adapt "in *trans*" using Cas1-2 machinery from other co-occurring CRISPR loci in the same genome. Adaptation in *trans* has been reported to accommodate spacer acquisition by the *Flavobacterium columnare* type VI-B system using co-resident type II-C Cas1-2, as well as by the *Klebsiella pneumoniae* type IV-A3 system using type I-E adaptation machinery.[22,23] However, the generality of this phenomenon and the mechanisms underlying orthogonal array selection by a single Cas1-2 remain unclear. Finally, the ability of some Cas1-2 machinery to install spacers in multiple distinct CRISPR loci raises the possibility that preexisting spacers in one CRISPR locus might prime adaptation into

Please cite this article in press as: Margolis and Meeske, Crosstalk between three CRISPR-Cas types enables primed type VI-A adaptation in *Listeria seeligeri*, Cell Host & Microbe (2025), https://doi.org/10.1016/j.chom.2025.05.020

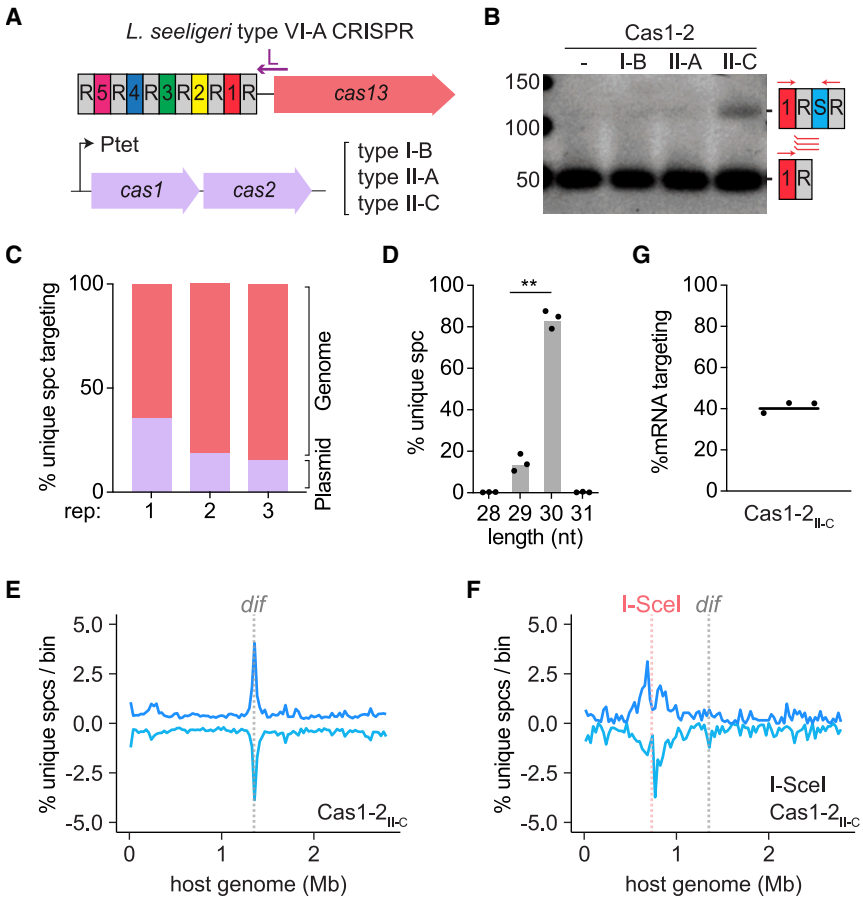

Figure 1. Type II-C Cas1-2 mediates type VI-A spacer acquisition

(A) Diagram of the experimental setup. Spacer acquisition was assayed in the native *L. seeligeri* type VI-A CRISPR locus during induction of different Cas1-Cas2 types from a plasmid. Spacers are numbered, and the orientation of the leader is noted. R, repeat; L, leader.

(B) Agarose gel showing the results of enrichment PCRs for new leader-adjacent spacers in the native type VI-A locus post Cas1-2 induction.

(C–G) Deep sequencing analysis of type VI-A spacers acquired during type II-C Cas1-2 induction. (C) Percentage of unique spacers mapped to the plasmid or the *L. seeligeri* genome for each replicate (rep). (D) Length of newly acquired spacers. Asterisks denote statistical significance ($p = 0.0048$) using a paired Student's t test (two-tailed). (E) Percentage of unique genome-mapped spacers acquired per 27,976 bp bin (1% of the genome). Spacers were acquired from every genomic region but are particularly enriched near the *dif* site (gray line). The combination of unique spacers from $n = 3$ replicates is shown. Positive values represent the top strand, while negative values represent the bottom strand. (F) Percentage of unique genome-mapped spacers acquired per bin after 24 h of both type II-C Cas1-2 and I-SceI induction in a strain engineered with an I-SceI cut site (pink line). The combination of unique spacers from $n = 3$ replicates is shown. (G) Percentage of unique genome targeting spacers that target mRNA.

other arrays, but this concept has not been experimentally investigated.

In this study, we investigated spacer acquisition by the RNA-targeting type VI-A CRISPR system in its native host *Listeria seeligeri*. Type VI CRISPR systems use the nuclease Cas13 to engage mRNAs with complementarity to the spacer regions of crRNAs, and in response, unleash nonspecific RNA degradation activity, leading to a state of cell dormancy that is incompatible with phage replication.[24,25] The *L. seeligeri* type VI-A system does not encode its own *cas1* or *cas2* genes, but our data indicate that it can acquire new spacers in *trans* using the Cas1-2 complex from a co-occurring type II-C system. Despite the RNA-targeting nature of type VI-A systems, we find that spacers are acquired from DNA in a transcription-independent manner, through a process that does not require the Cas13 nuclease. Flexibility in spacer acquisition is mediated by type II-C Cas1-2, which we find catalyzes promiscuous integration into type II and type VI arrays *in vitro*. Finally, we discovered that preexisting spacers in a third co-resident type I-B CRISPR locus strongly "cross-prime" type II-C Cas1-2 for spacer acquisition into the type VI-A locus. Our findings represent an unprecedented level of crosstalk between three CRISPR-Cas types in the same cell, raising the possibility that similarly complex interactions may govern CRISPR immunity in a wide range of microbes.

RESULTS

Type II-C Cas1 and Cas2 mediate type VI-A spacer acquisition

We investigated the mechanism of spacer acquisition by the natural type VI-A CRISPR host *L. seeligeri* strain LS1.[26] Like all *Listeria* type VI-A systems, the LS1 type VI-A CRISPR locus lacks *cas1* and *cas2* genes (Figures 1A and S1A; Table S1). However, of 111 *Listeria* genomes that harbor type VI-A loci, 93% encode one or more additional DNA-targeting CRISPR types that possess *cas1* and *cas2*, suggesting that adaptation in *trans* could mediate type VI-A spacer acquisition in these strains (Figure S1A and Table S1). For each of the three co-occurring CRISPR types (I-B, II-A, and II-C), we tested whether their cognate *cas1-2* alleles could stimulate the capture and integration of new spacers into the type VI-A array. In the case of type I-B CRISPR, we also co-expressed *cas4*, which is known to play roles in prespacer processing.[27,28] We induced *cas1-2* expression from a plasmid for 48 h during two serial passages and subsequently performed enrichment PCR to preferentially amplify newly acquired spacers in the *cas13*-proximal position of the type VI-A CRISPR array. In these experiments, only expression of type II-C *cas1-2* was sufficient to robustly stimulate spacer acquisition in the native type VI-A array (Figure 1B).

Please cite this article in press as: Margolis and Meeske, Crosstalk between three CRISPR-Cas types enables primed type VI-A adaptation in *Listeria seeligeri*, Cell Host & Microbe (2025), https://doi.org/10.1016/j.chom.2025.05.020

We note that the *Listeria* type II-C CRISPR locus is variably identified as type II-A or type II-C. While the locus does encode a highly divergent homolog of the type II-A signature gene *csn2*, the Cas9 protein sequence is more closely related to well-characterized Cas9c proteins than to Cas9a (Figure S1B) and is much smaller than most Cas9a proteins. Furthermore, our results demonstrate that the *csn2*-like gene in this system is not strictly required for spacer acquisition. As type II-A systems originated from within the type II-C phylogeny, the *Listeria* system and its relatives may represent a recombinant hybrid.[8] Due to the clear distinctions between this locus and the canonical type II-A locus present in *Listeria*, in addition to the difference in results between the systems in this work and others,[29–31] we refer to it as a type II-C locus.

To analyze the distribution of genomic sequences sampled during type VI-A spacer acquisition, we performed deep sequencing of the expanded array amplicons and mapped the results to both the *cas1-2* expression plasmid and the *L. seeligeri* genome (Figures 1C, S2A, and S2B). Most acquired spacers targeted the genome (Figure 1C). The vast majority of acquired spacers were 30 bp in length, with some shorter 29 bp spacers, consistent with the repertoire of native arrays (Figure 1D). To look for hotspots of acquisition, we split the *L. seeligeri* genome into 100 bins and counted the number of unique spacers targeting sequences in each bin (Figure 1E), which mitigates the impact of PCR bias. Spacers were acquired from most genomic regions, but there was a major enrichment of spacers targeting near the chromosomal terminus on both strands, as has been observed with type II-A spacer acquisition.[12,13] Specifically, the peak of spacers was centered at the 28 bp predicted *L. seeligeri dif* site, which differs from its experimentally verified equivalent in *Bacillus subtilis* by only a single nucleotide.[32] This enrichment is attributed to the double-stranded breaks (DSBs) that must occur at this site to resolve chromosomal dimers and concatemers prior to cell division. To determine whether DSBs are sufficient to cause type VI-A spacer acquisition, we engineered a unique 18 bp recognition site for the meganuclease I-SceI into the *L. seeligeri* genome, and induced expression of I-SceI along with type II-C Cas1-2 for 24 h. The vast majority of spacers acquired in this experiment targeted regions centered around the cut site (Figures 1F and S2C), indicating that these DNA ends are preferred acquisition substrates.

Because type VI CRISPR systems target RNA, transcriptionally silent regions of the genome would not serve to produce functional spacers. We compared the newly acquired spacer repertoire with annotated open reading frames (ORFs) to see whether functional, mRNA-targeting spacers were preferentially acquired (Figure 1G). In all experiments, less than 50% of acquired spacers targeted mRNA, indicating that there is no mechanism for selection of functional type VI-A spacers at the level of acquisition. We also considered that there could be some selection for functional spacers by acquiring preferentially from highly transcribed regions, as has been observed for type III-A CRISPR.[33] We compared the frequency of acquisition from each ORF with its read depth, calculated from a previous transcriptomic analysis,[25] and found no correlation between transcript levels and spacer acquisition (Figure S2D). We also compared levels of transcription in 1 or 10 kb bins with acquisition in those bins and again found no correlation (Figure S2D). These data indicate that in *L. seeligeri*, type VI-A spacers are not selected for mRNA-targeting ability when acquired via type II-C adaptation machinery. Coupled with our observation of spacer acquisition from DNA ends, these results strongly suggest that DNA, rather than mRNA, is the primary substrate for type VI-A adaptation.

Cas13 is not required for type VI-A spacer acquisition

How is the type II-C Cas1-2 complex recruited to integrate spacers into an orthogonal type VI-A array? As Cas13 is the only ORF in the type VI-A locus, we wondered whether Cas13 could play a role in spacer acquisition. We repeated the type II-C Cas1-2 induction experiments in strain backgrounds where either the nuclease activity of Cas13 was removed by inactivation of both HEPN (higher eukaryotes and prokaryotes nucleotide-binding) domains (dCas13) or where an early stop codon was introduced to make a Cas13 null ($Cas13_{Y80}$*). These Cas13 mutants were confirmed to be nonfunctional in target plasmid interference (Figure S3A). The absence of Cas13 had no detectable effect on the substrate source, length, distribution, or mRNA-targeting frequency of acquired spacers (Figures 2A–2D, S2E, S2F, S3B, and S3C), indicating that Cas13 is neither required for nor influences type VI-A spacer acquisition.

We were surprised to find that the presence of Cas13 had no impact on the frequency of mRNA-targeting spacers acquired (Figure 1G vs. Figure 2B). In principle, Cas13 should be activated by expressed target mRNAs, causing the cell to enter dormancy, and this effect should be abrogated with nonfunctional Cas13 alleles (dCas13 or $Cas13_{Y80}$*). These results could arise from insufficient target expression levels to trigger Cas13 activity[34]; detection of spacers originating from dormant yet intact cells in the culture; and/or inactivation of Cas13 in cells acquiring self-targeting spacers. We are unable to fully distinguish between these possibilities in bulk assays; however, we decided to test whether individual self-mRNA-targeting spacers acquired in this assay could lead to cell dormancy when the targeted transcripts are expressed at native levels. We cloned 13 individual spacers into a chromosomal type VI-A mini-array under its native promoter, introduced these into wild-type (WT) or $Cas13_{Y80}$* LS1 via conjugation, and plated for transconjugants (Figure S3D). Only 4 of the 13 spacers led to Cas13-dependent growth inhibition, and this was partially correlated with expression levels of the target from previously published studies. This indicates that many host transcripts are not abundant enough to be sensed by Cas13, while some crRNAs may be unstable or otherwise nonfunctional. These observations help explain how the acquisition of self-targeting spacers can be tolerated.

The *cas1-2* genes we expressed are derived from a type II-C CRISPR locus that also encodes Cas9c, which we reasoned could play a role in type VI-A spacer acquisition. We were unable to do experiments in a strain that natively contains both the type VI-A and type II-C systems, as these strains contain anti-CRISPR activity from an unidentified source that renders the type II-C system inactive.[31] Instead, we inserted the *cas9c* gene and its cognate tracrRNA into the LS1 chromosome, along with type II-C arrays containing 1 or 10 spacers, and repeated the type II-C Cas1-2 induction experiments. Under these conditions, type VI-A spacers were still acquired with patterns similar to those observed in the absence of *cas9* (Figures S3E and S3F),

Please cite this article in press as: Margolis and Meeske, Crosstalk between three CRISPR-Cas types enables primed type VI-A adaptation in *Listeria seeligeri*, Cell Host & Microbe (2025), https://doi.org/10.1016/j.chom.2025.05.020

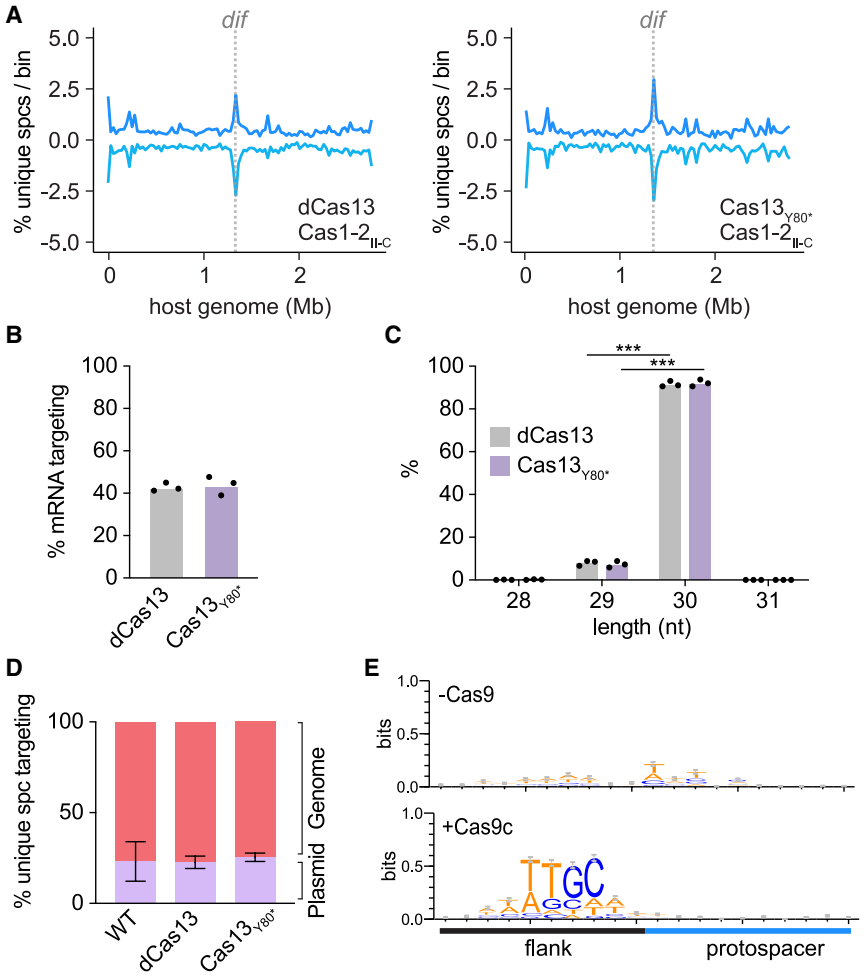

Figure 2. Contribution of Cas nucleases to type VI-A spacer acquisition

(A) Percentage of unique, genome-mapped type VI-A spacers acquired per bin during type II-C Cas1-2 induction in dCas13 (left) or $Cas13_{Y80^*}$ (right) mutants. The combination of unique spacers from $n = 3$ replicates is shown. Positive values represent the top strand, while negative values represent the bottom strand.

(B–D) Analysis of mRNA-targeting ability (B), length (C), and plasmid vs. genomic targets of newly acquired spacers from the experiment in (A). In (D), the data for the WT condition are the same as in Figure 1C. Asterisks denote statistical significance ($p < 0.001$) using a paired Student's t test (two-tailed).

(E) Sequence motif resulting from alignments of genome-mapped type VI-A spacer targets acquired during type II-C Cas1-2 expression, in the presence or absence of Cas9c. Each plot represents a combination of two biological replicates.

but the preponderance of newly acquired spacers matched target sequences flanked by a protospacer adjacent motif (PAM) identical to the reverse complement of natural type II-C targets (3' NNGCAA; Figure 2E). These data suggest that Cas9c participates in the type VI-A spacer acquisition process and is responsible for specifying a type II-C PAM. Our results extend the previous finding that type II-A Cas9 mediates the selection of targets with the correct PAM during adaptation[35] and are consistent with observations of type II-C PAMs during type VI-B spacer acquisition in *F. columnare*.[22] Altogether, these data indicate that in a strain with type II-C and VI-A CRISPR-Cas systems, the spacers acquired in the type VI-A locus follow the patterns of type II-C spacer acquisition.

Type II-C Cas1-2 integrates prespacers into type II and type VI arrays *in vitro*

Since Cas13 is not required to recruit the type II-C Cas1-2 complex to the type VI-A array, we reasoned that sequence similarities between the two arrays may allow either to be recognized by Cas1-2 for insertion of new spacers. The two arrays contain 36 bp direct repeat sequences sharing 54% nucleotide identity, spacers averaging 30 bp in length, and exhibit some similarity in the leader sequence, especially in the array-proximal region, which is important for directing the polarity of spacer acquisition in type II-A systems[36] (Figure 3A). To test whether type II-C Cas1-2 exhibits a preference for these arrays, we first separately expressed and purified the *L. seeligeri* type II-C Cas1 and Cas2 proteins from *E. coli* (Figure S4A). Next, we tested their ability to perform half-site integration into plasmids containing single-spacer type VI-A, II-A, II-C, and I-B arrays *in vitro* when supplied with dsDNA prespacer fragments containing 4 nt ssDNA overhangs on both ends[37] (Figure 3B). Half-site integration was assayed using one primer downstream of the array on the plasmid substrate and one primer matching the prespacer, such that preferential integration anywhere on the plasmid could be detected. Cas1-2 catalyzed half-site integration only into plasmids containing the type II-A, II-C, and VI-A arrays, and this occurred at the expected leader-repeat junction (Figures 3C and S4B; products were also confirmed by sequencing). The lack of integration into the control and type I-B array-containing plasmids indicates that the type II-C Cas1-2 complex has inherent specificity for the type II and type VI-A arrays. Next, we tested whether the leaders and/or repeats were required for integration by separately deleting the leader or repeat-spacer-repeat from plasmid substrates. Half-site integration was abrogated in both L- and RSR-only plasmids for both type II-C and type VI-A (Figures 3D and S4C), indicating that both the leader and repeats are required for prespacer integration *in vitro*. These experiments indicate that the *L. seeligeri* type II-C integration machinery exhibits inherent promiscuity with respect to array recognition and is sufficient to integrate dsDNA prespacers into type VI-A CRISPR arrays.

Acquisition of type VI-A spacers during phage infection

We wondered whether type II-C Cas1-2 expression would enable acquisition of protective type VI-A phage-targeting spacers during infection. We infected *L. seeligeri* cells

Please cite this article in press as: Margolis and Meeske, Crosstalk between three CRISPR-Cas types enables primed type VI-A adaptation in *Listeria seeligeri*, Cell Host & Microbe (2025), https://doi.org/10.1016/j.chom.2025.05.020

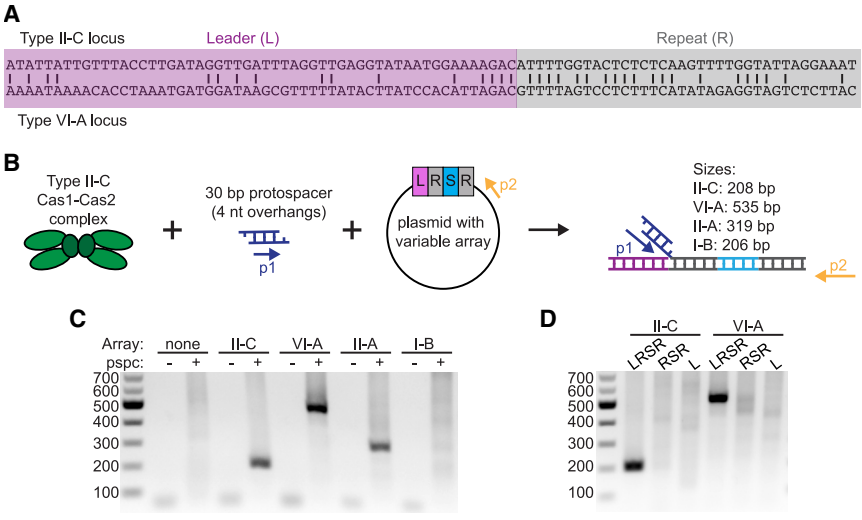

Figure 3. Type II-C Cas1-2 mediates half-site integration into type II and type VI-A arrays *in vitro*

(A) Comparison of the *L. seeligeri* type II-C and type VI-A leader and direct repeat sequences.

(B) Schematic of the assay to detect half-site integration by type II-C Cas1-2 *in vitro*. Purified Cas1-2 protein was incubated with a 30 bp prespacer (with 4 bp overhangs; pspc) and a plasmid with variable CRISPR arrays. The location of primers p1 and p2, as well as the expected sizes of the PCR product from leader-adjacent half-site integration into different arrays, are noted.

(C) Integration assay PCR on the indicated samples. Sizes are consistent with half-site integration at the leader-adjacent repeat for type II-C, type VI-A, and type II-A arrays. Samples without pspc were incubated with Cas1-2 and plasmid only. No array control contains the parental vector.

(D) Integration assay PCR with indicated type II-C or VI-A plasmids. LRSR, leader-repeat-spacer-repeat; RSR, array only; L, leader only.

(C and D) Results are representative of $n = 3$ experiments.

expressing type II-C Cas1-2 with the temperate listeriaphage U153 at an MOI (multiplicity of infection) of 0.1 and isolated genomic DNA 48 h post infection (hpi) from surviving cells. Most cells had not acquired a type VI-A spacer, indicating there are other ways for the cells to gain resistance to U153. Regardless, we deep-sequenced the expanded type VI-A arrays from each sample and mapped the acquired spacers to both the host and phage genomes. A disproportionate number of the type VI-A spacers detected in this experiment targeted the phage genome (Figure 4A; 2.8 Mb host genome vs. 42 kb phage genome), indicating that type II-C Cas1-2 can catalyze type VI-A adaptation to infecting phage, with no clear strand bias or subgenomic sites of enrichment (Figures 4B and S5B). To test whether any of the acquired spacers were functional, we cloned six individual phage-mRNA-targeting spacers from our experiment into a type VI-A mini-array in WT or $Cas13_{Y80}$* and infected lawns with U153 (Figure S6). All six spacers led to robust defense in the presence of WT Cas13. Thus, type VI-A spacers acquired via type II-C Cas1-2 can mediate type VI-A CRISPR-Cas defense.

Interestingly, a new spacer acquisition hotspot appeared in the host chromosome during U153 infection. This region corresponded to host genomic regions adjacent to the U153 prophage integration site, which is located within the *comK* gene[38] (Figures 4C and S5A). These results raised the possibility that prophage integration stimulates spacer acquisition, as it is a process that involves DSB formation.[39] To test this, we constructed a lytic U153 phage mutant ($U153_{lyt}$) lacking the lysogenic operon and repeated the infection and acquisition experiments. Spacers targeting the lytic mutant were acquired at the same rate as WT phage, but we no longer observed strong enrichment of spacers originating from near the prophage integration site (Figures 4A, 4D, 4E, S5C, and S5D). This demonstrates that type VI-A spacers can be acquired during lytic infection. However, it remained unclear whether spacers were acquired from near the prophage integration site during lysogen establishment or from an already integrated prophage. To test this, we isolated U153 lysogens, induced type II-C Cas1-2, and monitored acquisition of new spacers in the type VI-A array. Under these conditions, we observed a dominant peak of newly acquired type VI-A spacers targeting the prophage and surrounding regions of the host genome (Figures 4F and S5E), which was completely dependent on type II-C Cas1-2 expression (Figure S5F). We reasoned that spacer acquisition from the prophage could be explained by spontaneous prophage reactivation by a subpopulation of the cells in the culture, followed by prophage excision and subsequent phage genome injection into neighboring lysogens. To investigate this, we deleted the integrase gene from the prophage, which impaired its ability to produce viable plaque-forming units (PFUs) by 5 orders of magnitude during prophage induction (Figure S5G). Surprisingly, when we repeated the type II-C Cas1-2 induction experiments in the lysogen harboring Δ*int* prophage, we observed an equally strong enrichment of type VI-A spacers targeting the prophage and surrounding regions (Figures 4G and S5H). That spacers were acquired from this inert "locked-in" prophage mutant suggests that some property of the U153 sequence itself, rather than the phage life cycle, strongly stimulates spacer acquisition.

Type I-B CRISPR primes type II-C Cas1-2 for type VI-A spacer acquisition

The experimental strain of *L. seeligeri* we used for our assays (LS1) contains, in addition to a native type VI-A locus, a type I-B CRISPR-Cas locus that is largely transcriptionally silent under laboratory growth conditions (Figures S7A and S7B), and does not interfere against plasmids containing matching protospacers (Figure S7C). However, this type I-B system has previously been shown to be functional when expressed under the control of an inducible promoter, and thus the lack of activity seems to be due to low expression levels.[31] Upon further analysis, we noticed that this type I-B locus contains one natural spacer that targets the U153 genome with a single mismatch (Figure 5A). This native type I-B locus does not offer any protection during U153 infection (Figure 5B), as WT LS1 and a mutant lacking the entire type I-B

Please cite this article in press as: Margolis and Meeske, Crosstalk between three CRISPR-Cas types enables primed type VI-A adaptation in *Listeria seeligeri*, Cell Host & Microbe (2025), https://doi.org/10.1016/j.chom.2025.05.020

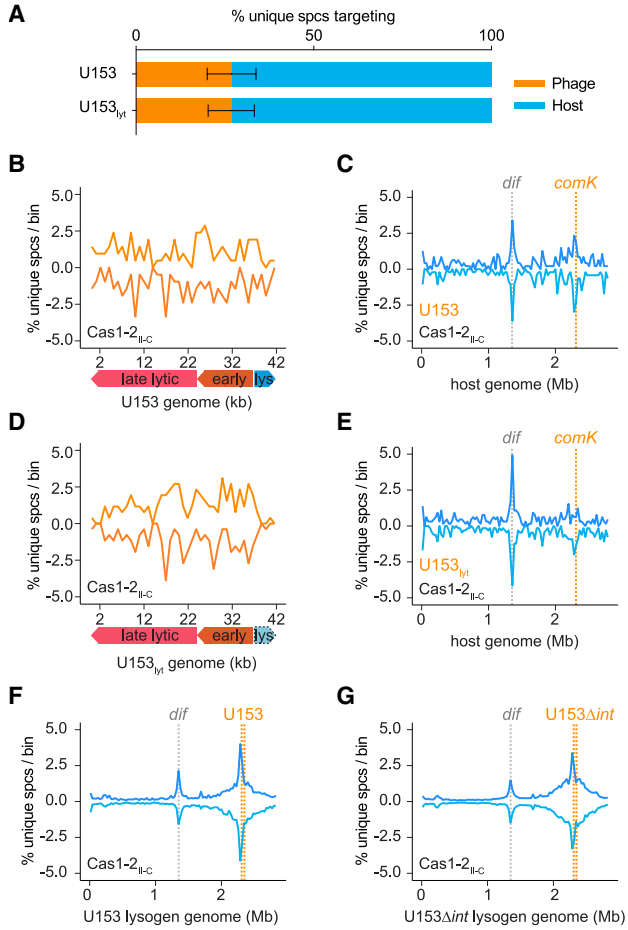

Figure 4. Acquisition of phage-targeting type VI-A spacers during type II-C Cas1-2 induction

(A) Percentage of unique acquired spacers targeting the host or phage genome during infection with U153 phage or strictly lytic mutant ($U153_{lyt}$) in cells expressing type II-C Cas1-2.

(B–E) Percentage of unique spacers per bin from the experiment described in (A), mapped to the phage (B andD) and host (C and E) genomes. The combination of unique spacers from $n = 3$ replicates is shown. In (B) and (D), the bin size is 986 bp; in (C) and (E), the bin size is 1% of the host genome. Prophage integration site *comK* (orange) and *dif* site (gray) are indicated. (B and C) Spacers acquired during WT U153 infection, where some infection events may result in prophage integration. (D and E) Spacers acquired during infection with $U153_{lyt}$, which lacks integration machinery.

(F and G) Percentage of unique lysogen genome-mapped type VI-A spacers acquired per bin (1% of the lysogen genome) during type II-C Cas1-2 induction. The combination of unique spacers from $n = 3$ replicates is shown. Boundaries of the integrated prophage are shown (orange). (F) Spacers acquired in the WT U153 lysogen, where the prophage can potentially reactivate. (G) Spacers acquired in the U153Δ*int* lysogen, in which the U153 integrase gene has been knocked out of the lysogen genome, largely removing the prophage's ability to excise.

CRISPR-Cas locus are equally permissive to phage infection. We hypothesized that in a subpopulation of cells, or at some low level, the type I-B system is expressed and able to use this U153-targeting spacer to prime type VI-A spacer acquisition through type II-C Cas1-2, leading to the enrichment of prophage-targeting spacers we observe in Figures 4F and 4G. To explore this possibility, we lysogenized mutants lacking the entire type I-B CRISPR-Cas locus with U153 and repeated the spacer acquisition experiments with induction of type II-C Cas1-2. In the mutants, spacers targeting the prophage and surrounding genome were no longer preferentially acquired in the type VI-A array (Figures 5C, 5D, S8A, and S8B), supporting the hypothesis that type I-B cross-primes type VI-A acquisition. Notably, type VI-A spacers targeting near the *dif* site were acquired in both the WT and Δtype I-B mutant, suggesting that the role of type I-B in type VI adaptation is specific to priming. We wondered whether type I-B was required for acquisition of type VI-A spacers during U153 infection, so we repeated the infection experiments with type II-C Cas1-2 induction in the Δtype I-B mutant (Figure S8C). Phage-targeting type VI-A spacers were still acquired, indicating that type I-B priming is not strictly required for type VI-A adaptation to phage.

Type I priming requires the helicase-nuclease Cas3, which is thought to interact with type I Cas1-2 and aid in processing new prespacers from near the target. To understand the requirements of type I-B cross-priming of type VI-A adaptation through the type II-C acquisition machinery, we deleted either the endogenous type I-B Cas3 or Cas1 and Cas2 from the LS1 genome (Figure S7A), lysogenized the mutants with U153, and repeated spacer acquisition experiments with induction of type II-C Cas1-2. Primed spacer acquisition was completely dependent on type I-B Cas3 (Figures 5E and S8E) but not on type I-B Cas1-2 (Figures 5F and S8D), confirming that type II-C Cas1-2 are solely responsible for spacer integration. We then wondered whether the nuclease activity of Cas3 was required for cross-priming, as in other systems, it cleaves DNA into prespacer fragments. We generated mutations (H49A and D50A) in the nuclease domain of the *cas3* gene in LS1 ($Cas3_{mut}$) and repeated the acquisition assays in the presence of the U153 prophage and type II-C Cas1-2 (Figure 5G). Primed acquisition was completely dependent on the nuclease activity of Cas3.

Finally, to test whether a type I-B spacer is sufficient to prime type VI-A acquisition by type II-C CRISPR, we ectopically integrated a type I-B spacer targeting the host genome with a single mismatch under the native type I-B array promoter and repeated the type II-C Cas1-2 induction experiments. Strikingly, we observed the emergence of a new hotspot of type VI-A spacers mapping near the engineered type I-B target site (Figures 5H and S8F), which was dependent on the presence of Cas3 (Figures 5I and S8G), the Cas3 nuclease activity (Figure 5J), and the native type I-B CRISPR-Cas system (Figure S8H). Altogether, these data indicate that type I-B CRISPR can prime the type II-C Cas1-2 integrase to capture and integrate new spacers into the type VI-A CRISPR array.

Generality of type VI adaptation in *trans* and cross-priming

We next searched for bioinformatic signatures of the type VI adaptation in *trans* and cross-priming phenomena observed in this study in other genomes beyond *L. seeligeri*. To this end, we analyzed the frequency of adaptation gene occurrence in type VI CRISPR loci, co-occurrence with other CRISPR types, and the existence of adaptation genes in co-occurring CRISPR systems. We analyzed the CRISPR-Cas content of all 1,089 publicly available Cas13-containing genomes from NCBI (Table S1). Over 77% of type-VI-containing genomes in our analysis also contain another

Please cite this article in press as: Margolis and Meeske, Crosstalk between three CRISPR-Cas types enables primed type VI-A adaptation in *Listeria seeligeri*, Cell Host & Microbe (2025), https://doi.org/10.1016/j.chom.2025.05.020

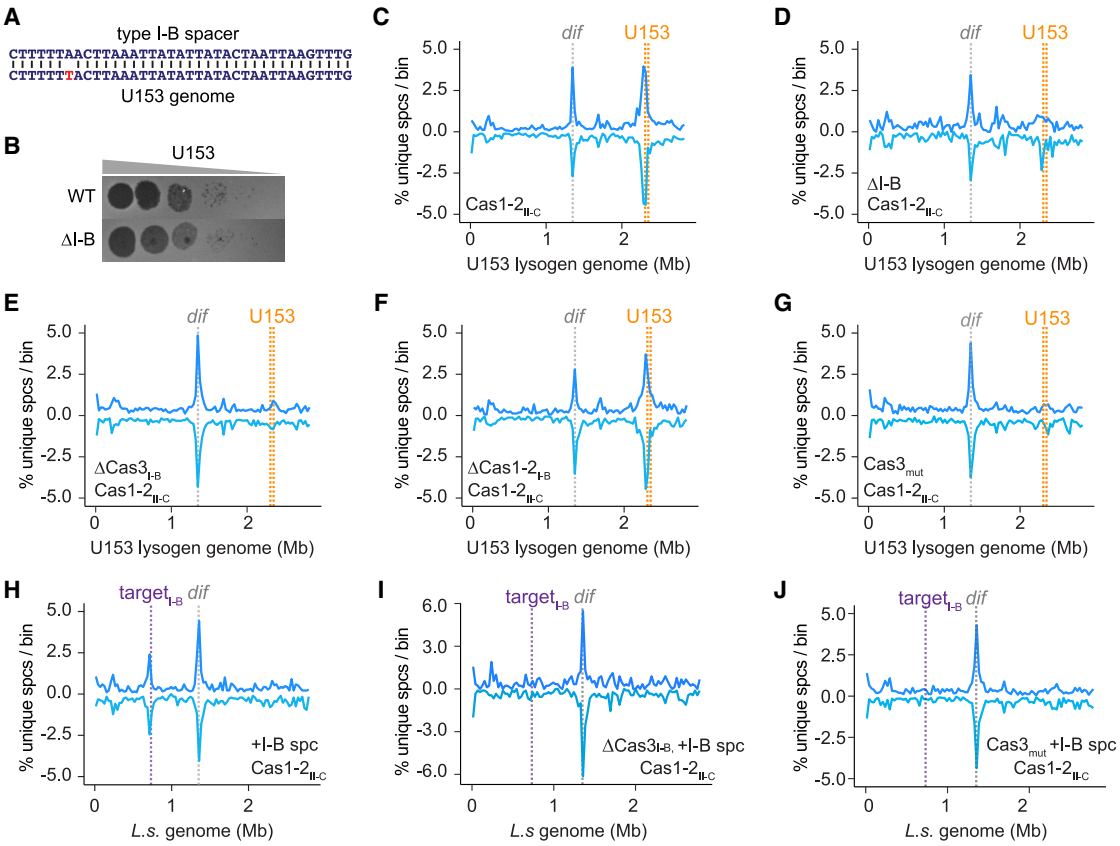

Figure 5. Type I-B CRISPR primes type II-C Cas1-2 for type VI-A spacer acquisition

(A) Comparison of a type I-B spacer that exists in the LS1 genome with a sequence in the U153 genome. A single mismatch is highlighted in red.

(B) U153 infection of lawns of WT LS1 or LS1 lacking the entire type I-B locus (ΔI-B). Representative of $n = 3$ experiments.

(C–G) Percentage of unique lysogen-genome-mapped type VI-A spacers acquired per 1% bin during type II-C Cas1-2 induction. The combination of unique spacers from $n = 2$ replicates is shown. Boundaries of the integrated prophage (orange) and the *dif* site (gray) are shown. (C) Spacers acquired in WT U153 lysogens, as in Figure 4F, but from two distinct biological replicates completed alongside the experiments shown in (D) and (E). (D) Spacers acquired in ΔI-B U153 lysogens. (E) Spacers acquired in U153 lysogens lacking the Cas3 gene in the type I-B locus. (F) Spacers acquired in U153 lysogens lacking the Cas1 and Cas2 genes in the type I-B locus. (G) Spacers acquired in U153 lysogens with inactivating point mutations in the nuclease domain of Cas3 (H49A and D50A; referred to as $Cas3_{mut}$).

(H–J) Percentage of unique genome-mapped spacers acquired per 1% bin during type II-C Cas1-2 induction in the presence of a type I-B spacer targeting a genomic location (purple) with a single mismatch. The combination of unique spacers from $n = 2$ replicates is shown. (H) Spacers acquired in WT LS1. (I) Spacers acquired in $\Delta Cas3_{I-B}$ LS1. (J) Spacers acquired in $Cas3_{mut}$ LS1.

CRISPR type, and interestingly, type II-C was one of the most frequently co-occurring systems with type VI, despite its relative rarity[8] (Figure 6A). Furthermore, we found that type II-C CRISPR repeats often share sequence similarity and have the same length as co-occurring type VI repeats (Figures S1C and S1D). The vast majority of CRISPR types co-occurring with type VI encode both Cas1 and Cas2 genes (Figure 6B), while these are largely absent from the type VI loci (Figure 6C). Thus, the majority of known type VI systems do not encode Cas1-2 but are present in a genome that contains these acquisition genes, meeting the requirements for potential acquisition in *trans*.

Our experimental data also uncovered the phenomenon of cross-priming, where spacers in one CRISPR locus prime the generation of spacers for a different CRISPR type. One prediction of cross-priming is that spacers from different CRISPR types in the same genome would target the same phage or other mobile genetic element (MGE). While there are other mechanisms by which this could occur (discussed below), we looked for this signature of cross-priming by searching for spacer targets for all CRISPR loci in type-VI-containing genomes. We limited subsequent analysis to the 441 genomes that possessed a second CRISPR type and for which type VI spacer targets were detected. We found that over 2/3 of the genomes had at least one type VI spacer that shares a putative target with a spacer from another co-occurring CRISPR type (Figure 6D and Table S1). These observations support the idea that cross-priming is a common mechanism of spacer acquisition.

DISCUSSION

In this study, we sought to understand how a type VI-A CRISPR system can acquire new spacers without encoding its own Cas1 and Cas2 machinery. We found that in *L. seeligeri*, type II-C Cas1 and Cas2 can integrate new spacers into the native type VI-A

Please cite this article in press as: Margolis and Meeske, Crosstalk between three CRISPR-Cas types enables primed type VI-A adaptation in *Listeria seeligeri*, Cell Host & Microbe (2025), https://doi.org/10.1016/j.chom.2025.05.020

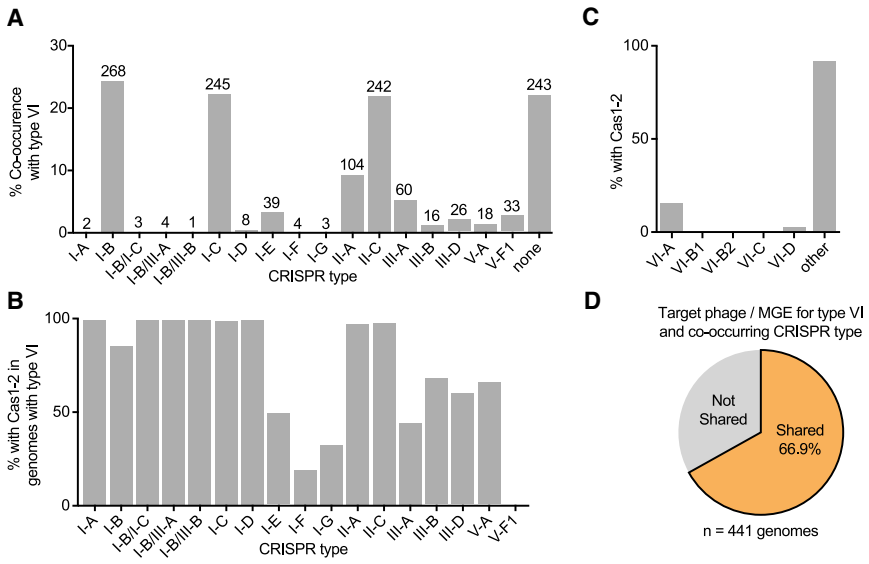

Figure 6. Co-occurrence of type VI with adaptation-competent CRISPR systems

(A) All 1,089 publicly available Cas13-containing genomes were analyzed by CRISPRCasTyper to determine the frequency of co-occurring CRISPR types. The number of genomes containing each CRISPR type is indicated above the bar.

(B) Frequency with which each co-occurring CRISPR type in (A) encodes Cas1 and Cas2 genes.

(C) Frequency with which different type VI subtypes encode Cas1 and Cas2. 92% of type VI-containing genomes that have another CRISPR type do encode Cas1-2 from another CRISPR locus.

(D) Result of spacer target analysis. Targets for all spacers in all type-VI-containing genomes were identified by probing the IMGVR, IMGPR, MGV, and GPD databases. Genomes that contained a non-type VI CRISPR locus and for which at least one type VI spacer match was identified were analyzed for putative target sharing. 295 of 441 genomes contained a type VI and a non-type VI spacer that share a putative target.

locus. Type VI CRISPR acquisition using the type II-C integrase complex has previously been reported in the distantly related type VI-B system of *F. columnare*, where the type II-C Cas1 and Cas2 are only 33% and 37% identical to the *L. seeligeri* system, respectively. This suggests that the promiscuity of type II-C Cas1-2 enzymes, or of type VI arrays, may be a widespread phenomenon. Indeed, we found that over 22% of type VI systems co-occur with type II-C despite type II-C systems being present in only ~7% of bacterial genomes.[8] Almost all of these co-occurring type II-C systems have Cas1-2 (98%), so it may be common for type VI CRISPR to acquire spacers in *trans* using Cas1-2 from type II-C. We also found that the type II-C Cas1-2 enzymes from *L. seeligeri* were sufficient to integrate prespacers into the type VI-A array *in vitro*, and this was dependent on the leader sequences, despite limited sequence similarity between the type II-C and VI-A leaders. Thus, type II-C spacer integrases may have relaxed specificity for array recognition and integration, which is co-opted for type VI-A spacer acquisition.

During this study, we also serendipitously discovered a role for type I-B priming in type VI-A spacer acquisition by using a phage that has a single mismatch to a spacer natively present in the *L. seeligeri* type I-B array. While this spacer does not provide broad protection during infection (Figure 5B), it is able to prime type II-C Cas1-2 to capture spacers near the mismatched target and integrate them into the type VI-A array. During type I priming, Cascade recruits type I Cas1-2 to mismatched targets[18]; perhaps it is able to physically interact with divergent type II-C Cas1-2 machinery as well. Alternatively, target recognition by the priming spacer could stimulate a low level of target DNA cleavage by Cas3, which would supply linear DNA ends to serve as spacer acquisition substrates. We found that cross-priming was entirely dependent on the nuclease activity of Cas3, so Cas3 is likely playing a role in the generation of prespacer fragments, which may or may not be coordinated with Cas1-2. The extent of such "cross-priming" between distinct CRISPR types in the same genome remains an outstanding question. To look for evidence of cross-priming in nature, we searched for spacers from different CRISPR types in the same genome targeting the same MGE. This analysis is complicated by the fact that (1) many spacer targets are unknown and (2) many putative target sequences are shared between MGEs, making it difficult to assign an origin of acquisition. In addition, spacer targets could be shared due to parallel acquisition events during infection rather than cross-priming. Nonetheless, our analysis of type VI-containing genomes found that over 2/3 of type VI loci shared at least one target with another CRISPR type in the genome, arguing that cross-priming could be a significant player in type VI acquisition. The phenomenon of cross-priming requires either Cas1-2 machinery that can act in *trans* on multiple CRISPR arrays or communication between the priming CRISPR system and multiple distinct Cas1-2 complexes. In this study, we have demonstrated that both mechanisms exist and could provide a path for rapid dissemination of established immunological memories across CRISPR-Cas loci.

As functional PAM sequences are selected during the spacer acquisition process, relatively PAM-flexible RNA-sensing type III and type VI CRISPR systems are well-poised to receive spacers from orthogonal Cas1-2 machinery acting in *trans*. A previous analysis of spacer targets found that in type III CRISPR systems that do not encode their own cas1-2 genes, most spacer targets have a PAM, likely due to acquisition *in trans* from co-occurring type I CRISPR systems.[40] Notably, acquisition in *trans* would not be as advantageous for DNA-targeting CRISPR types, as these require precise PAM matches to identify a target. Cross-priming might be particularly advantageous in the event of infection by a phage refractory to targeting by the priming CRISPR type, due to the expression of anti-CRISPRs or other resistance mechanisms, such as DNA modifications.[41] In these cases, the interference machinery of one CRISPR type may be inhibited, but as long as spacer acquisition can occur, interference can be achieved through a co-occurring CRISPR type. It has also been shown that some type III CRISPR systems can mediate interference using type I crRNAs, enabling robust protection against phages containing target site mutations.[42] Taken

together, these and our findings indicate that distinct co-resident CRISPR types can influence each other at all levels of immunity.

It is worth noting that during cross-priming in the U153 lysogen, all acquired spacers are self-targeting, despite the priming spacer targeting a phage-derived sequence. In DNA-targeting CRISPR systems, this would not be advantageous, as newly acquired prophage-matching spacers could then be used to target and cleave the host genome. However, type VI CRISPR systems sense RNA, and therefore, the target must be transcribed to trigger Cas13 activity. Prophages do not express the majority of their genes, as these make proteins involved in replication and lysis. However, upon reactivation, these lytic mRNAs are again produced. Thus, if a type VI spacer targeting a lytic mRNA of the prophage were acquired through the priming mechanism discovered in this study, this immune system would be "off" until the phage reactivates. This mechanism could potentially allow a cell to maintain beneficial genes present in a prophage but stop it from reactivating and lysing the cell.

Why do so few type VI CRISPR systems encode Cas1 and Cas2 genes? We propose that it may be evolutionarily advantageous to couple the acquisition of type VI spacers with the presence of a DNA-targeting immune system, such as type I or II CRISPR. Type VI CRISPR activation leads to cell dormancy, and as long as the activating mRNA target is present, the cell will not escape dormancy. However, we have previously shown that in the presence of restriction-modification systems, cells that have undergone Cas13-mediated dormancy can be resuscitated due to destruction of the phage DNA that is transcribed to produce the activating mRNA.[43] Perhaps using Cas1-2 from a DNA-targeting system gives cells with type VI immunity a better chance to exit dormancy if this machinery is also used to acquire DNA-targeting spacers from the same target. Further studies will be needed to shed light on the advantages and disadvantages of harboring multiple CRISPR systems that can interact with each other.

Limitations of the study

While our study of type VI-A spacer acquisition was performed in the native host *L. seeligeri*, our adaptation assays relied on overexpression of type II-C Cas1-2, without which we were unable to detect spacer acquisition. Thus, while our data demonstrate that type II-C Cas1-2 can capture new spacers and integrate them into the type VI-A CRISPR array if sufficiently expressed, the extent to which this phenomenon occurs under truly native conditions remains to be determined.

RESOURCE AVAILABILITY

Lead contact

Requests for further information and resources should be directed to and will be fulfilled by the lead contact, Alexander J. Meeske (meeske@uw.edu).

Materials availability

All reagents generated in this study are available from the lead contact without restriction.

Data and code availability

- All raw sequencing data have been uploaded to the Sequence Read Archive Accession: PRJNA1246610.
- This paper does not report original code.
- Any additional information required to reanalyze the data reported in this paper is available from the lead contact upon request.

ACKNOWLEDGMENTS

We thank Marshall Godsil for finishing the construction of U153-cmR and for providing especially helpful suggestions. We also thank Monica Guo for help with protein purification, and Albina Kozlova, J.C. Alexander, and David Brinkley for their previous work on detecting type VI-A spacer acquisition. We would also like to thank all members of the Meeske lab for helpful discussions. Work in the Meeske lab is supported by NIGMS (R35GM142460), NSF (FAIN2235762), and the University of Washington Royalty Research Fund. S.R.M. is a Jane Coffin Childs Memorial Foundation Postdoctoral Fellow. A.J.M. is a Rita Allen Foundation Scholar.

AUTHOR CONTRIBUTIONS

The study was conceived by S.R.M. and A.J.M. S.R.M. performed all experiments described in the paper. S.R.M. and A.J.M. wrote and edited the paper.

DECLARATION OF INTERESTS

A.J.M. is a co-founder and advisor of Profluent Bio.

STAR★METHODS

Detailed methods are provided in the online version of this paper and include the following:

- KEY RESOURCES TABLE
- EXPERIMENTAL MODEL DETAILS
  - Bacterial strains and growth conditions
  - Phage propagation
- METHOD DETAILS
  - Plasmid construction
  - E. coli–L. seeligeri conjugation
  - Cas1-2 induction experiments
  - Sample preparation and array amplification for next-generation sequencing
  - Gene deletions
  - Cas1 and Cas2 purification
  - *In vitro* integration assays
  - Phage infections
  - U153-cmR construction
  - Bioinformatic analysis of CRISPR loci
  - Cas9 phylogenetic tree construction
- QUANTIFICATION AND STATISTICAL ANALYSIS
  - High throughput sequencing data analysis

SUPPLEMENTAL INFORMATION

Supplemental information can be found online at https://doi.org/10.1016/j.chom.2025.05.020.

Received: October 22, 2024
Revised: April 4, 2025
Accepted: May 16, 2025

REFERENCES

1. Barrangou, R., Fremaux, C., Deveau, H., Richards, M., Boyaval, P., Moineau, S., Romero, D.A., and Horvath, P. (2007). CRISPR provides acquired resistance against viruses in prokaryotes. Science *315*, 1709–1712. https://doi.org/10.1126/science.1138140.
2. Brouns, S.J.J., Jore, M.M., Lundgren, M., Westra, E.R., Slijkhuis, R.J.H., Snijders, A.P.L., Dickman, M.J., Makarova, K.S., Koonin, E.V., and van

der Oost, J. (2008). Small CRISPR RNAs guide antiviral defense in prokaryotes. Science *321*, 960–964. https://doi.org/10.1126/science.1159689.

3. Hale, C., Kleppe, K., Terns, R.M., and Terns, M.P. (2008). Prokaryotic silencing (psi)RNAs in Pyrococcus furiosus. RNA *14*, 2572–2579. https://doi.org/10.1261/rna.1246808.
4. Marraffini, L.A., and Sontheimer, E.J. (2008). CRISPR interference limits horizontal gene transfer in staphylococci by targeting DNA. Science *322*, 1843–1845. https://doi.org/10.1126/science.1165771.
5. Garneau, J.E., Dupuis, M.È., Villion, M., Romero, D.A., Barrangou, R., Boyaval, P., Fremaux, C., Horvath, P., Magadán, A.H., and Moineau, S. (2010). The CRISPR/Cas bacterial immune system cleaves bacteriophage and plasmid DNA. Nature *468*, 67–71. https://doi.org/10.1038/nature09523.
6. McGinn, J., and Marraffini, L.A. (2019). Molecular mechanisms of CRISPR-Cas spacer acquisition. Nat. Rev. Microbiol. *17*, 7–12. https://doi.org/10.1038/s41579-018-0071-7.
7. Makarova, K.S., Wolf, Y.I., Iranzo, J., Shmakov, S.A., Alkhnbashi, O.S., Brouns, S.J.J., Charpentier, E., Cheng, D., Haft, D.H., Horvath, P., et al. (2020). Evolutionary classification of CRISPR-Cas systems: a burst of class 2 and derived variants. Nat. Rev. Microbiol. *18*, 67–83. https://doi.org/10.1038/s41579-019-0299-x.
8. Makarova, K.S., Wolf, Y.I., Alkhnbashi, O.S., Costa, F., Shah, S.A., Saunders, S.J., Barrangou, R., Brouns, S.J.J., Charpentier, E., Haft, D.H., et al. (2015). An updated evolutionary classification of CRISPR-Cas systems. Nat. Rev. Microbiol. *13*, 722–736. https://doi.org/10.1038/nrmicro3569.
9. Ruffolo, J.A., Nayfach, S., Gallagher, J., Bhatnagar, A., Beazer, J., Hussain, R., Russ, J., Yip, J., Hill, E., Pacesa, M., et al. (2024). Design of highly functional genome editors by modeling the universe of CRISPR-Cas sequences. Preprint at bioRxiv. https://doi.org/10.1101/2024.04.22.590591.
10. Yosef, I., Goren, M.G., and Qimron, U. (2012). Proteins and DNA elements essential for the CRISPR adaptation process in Escherichia coli. Nucleic Acids Res. *40*, 5569–5576. https://doi.org/10.1093/nar/gks216.
11. Nunez, J.K., Kranzusch, P.J., Noeske, J., Wright, A.V., Davies, C.W., and Doudna, J.A. (2014). Cas1-Cas2 complex formation mediates spacer acquisition during CRISPR-Cas adaptive immunity. Nat. Struct. Mol. Biol. *21*, 528–534. https://doi.org/10.1038/nsmb.2820.
12. Levy, A., Goren, M.G., Yosef, I., Auster, O., Manor, M., Amitai, G., Edgar, R., Qimron, U., and Sorek, R. (2015). CRISPR adaptation biases explain preference for acquisition of foreign DNA. Nature *520*, 505–510. https://doi.org/10.1038/nature14302.
13. Modell, J.W., Jiang, W., and Marraffini, L.A. (2017). CRISPR-Cas systems exploit viral DNA injection to establish and maintain adaptive immunity. Nature *544*, 101–104. https://doi.org/10.1038/nature21719.
14. Deveau, H., Barrangou, R., Garneau, J.E., Labonté, J., Fremaux, C., Boyaval, P., Romero, D.A., Horvath, P., and Moineau, S. (2008). Phage response to CRISPR-encoded resistance in Streptococcus thermophilus. J. Bacteriol. *190*, 1390–1400. https://doi.org/10.1128/JB.01412-07.
15. Swarts, D.C., Mosterd, C., van Passel, M.W.J., and Brouns, S.J.J. (2012). CRISPR interference directs strand specific spacer acquisition. PLoS One *7*, e35888. https://doi.org/10.1371/journal.pone.0035888.
16. Datsenko, K.A., Pougach, K., Tikhonov, A., Wanner, B.L., Severinov, K., and Semenova, E. (2012). Molecular memory of prior infections activates the CRISPR/Cas adaptive bacterial immunity system. Nat. Commun. *3*, 945. https://doi.org/10.1038/ncomms1937.
17. Fineran, P.C., Gerritzen, M.J.H., Suárez-Diez, M., Künne, T., Boekhorst, J., van Hijum, S.A.F.T., Staals, R.H.J., and Brouns, S.J.J. (2014). Degenerate target sites mediate rapid primed CRISPR adaptation. Proc. Natl. Acad. Sci. USA *111*, E1629–E1638. https://doi.org/10.1073/pnas.1400071111.
18. Redding, S., Sternberg, S.H., Marshall, M., Gibb, B., Bhat, P., Guegler, C.K., Wiedenheft, B., Doudna, J.A., and Greene, E.C. (2015). Surveillance and Processing of Foreign DNA by the Escherichia coli CRISPR-Cas System. Cell *163*, 854–865. https://doi.org/10.1016/j.cell.2015.10.003.
19. Künne, T., Kieper, S.N., Bannenberg, J.W., Vogel, A.I.M., Miellet, W.R., Klein, M., Depken, M., Suarez-Diez, M., and Brouns, S.J.J. (2016). Cas3-Derived Target DNA Degradation Fragments Fuel Primed CRISPR Adaptation. Mol. Cell *63*, 852–864. https://doi.org/10.1016/j.molcel.2016.07.011.
20. Dillard, K.E., Brown, M.W., Johnson, N.V., Xiao, Y., Dolan, A., Hernandez, E., Dahlhauser, S.D., Kim, Y., Myler, L.R., Anslyn, E.V., et al. (2018). Assembly and Translocation of a CRISPR-Cas Primed Acquisition Complex. Cell *175*, 934–946.e15. https://doi.org/10.1016/j.cell.2018.09.039.
21. Nussenzweig, P.M., McGinn, J., and Marraffini, L.A. (2019). Cas9 Cleavage of Viral Genomes Primes the Acquisition of New Immunological Memories. Cell Host Microbe *26*, 515–526.e6. https://doi.org/10.1016/j.chom.2019.09.002.
22. Hoikkala, V., Ravantti, J., Díez-Villaseñor, C., Tiirola, M., Conrad, R.A., McBride, M.J., Moineau, S., and Sundberg, L.R. (2021). Cooperation between Different CRISPR-Cas Types Enables Adaptation in an RNA-Targeting System. mBio *12*, e03338-20. https://doi.org/10.1128/mBio.03338-20.
23. Benz, F., Camara-Wilpert, S., Russel, J., Wandera, K.G., Čepaitė, R., Ares-Arroyo, M., Gomes-Filho, J.V., Englert, F., Kuehn, J.A., Gloor, S., et al. (2024). Type IV-A3 CRISPR-Cas systems drive inter-plasmid conflicts by acquiring spacers in trans. Cell Host Microbe *32*, 875–886.e9. https://doi.org/10.1016/j.chom.2024.04.016.
24. Abudayyeh, O.O., Gootenberg, J.S., Konermann, S., Joung, J., Slaymaker, I.M., Cox, D.B.T., Shmakov, S., Makarova, K.S., Semenova, E., Minakhin, L., et al. (2016). C2c2 is a single-component programmable RNA-guided RNA-targeting CRISPR effector. Science *353*, aaf5573. https://doi.org/10.1126/science.aaf5573.
25. Meeske, A.J., Nakandakari-Higa, S., and Marraffini, L.A. (2019). Cas13-induced cellular dormancy prevents the rise of CRISPR-resistant bacteriophage. Nature *570*, 241–245. https://doi.org/10.1038/s41586-019-1257-5.
26. Rocourt, J., and Grimont, P.A.D. (1983). Listeria welshimeri sp. nov. and Listeria seeligeri sp. nov. Int. J. Syst. Evol. Microbiol. *33*, 866–869. https://doi.org/10.1099/00207713-33-4-866.
27. Shiimori, M., Garrett, S.C., Graveley, B.R., and Terns, M.P. (2018). Cas4 Nucleases Define the PAM, Length, and Orientation of DNA Fragments Integrated at CRISPR Loci. Mol. Cell *70*, 814–824.e6. https://doi.org/10.1016/j.molcel.2018.05.002.
28. Lee, H., Zhou, Y., Taylor, D.W., and Sashital, D.G. (2018). Cas4-Dependent Prespacer Processing Ensures High-Fidelity Programming of CRISPR Arrays. Mol. Cell *70*, 48–59.e5. https://doi.org/10.1016/j.molcel.2018.03.003.
29. Osuna, B.A., Karambelkar, S., Mahendra, C., Christie, K.A., Garcia, B., Davidson, A.R., Kleinstiver, B.P., Kilcher, S., and Bondy-Denomy, J. (2020). Listeria Phages Induce Cas9 Degradation to Protect Lysogenic Genomes. Cell Host Microbe *28*, 31–40.e9. https://doi.org/10.1016/j.chom.2020.04.001.
30. Hupfeld, M., Trasanidou, D., Ramazzini, L., Klumpp, J., Loessner, M.J., and Kilcher, S. (2018). A functional type II-A CRISPR-Cas system from Listeria enables efficient genome editing of large non-integrating bacteriophage. Nucleic Acids Res. *46*, 6920–6933. https://doi.org/10.1093/nar/gky544.
31. Katz, M.A., Sawyer, E.M., Oriolt, L., Kozlova, A., Williams, M.C., Margolis, S.R., Johnson, M., Bondy-Denomy, J., and Meeske, A.J. (2024). Diverse viral cas genes antagonize CRISPR immunity. Nature *634*, 677–683. https://doi.org/10.1038/s41586-024-07923-x.
32. Sciochetti, S.A., Piggot, P.J., and Blakely, G.W. (2001). Identification and characterization of the dif Site from Bacillus subtilis. J. Bacteriol. *183*, 1058–1068. https://doi.org/10.1128/JB.183.3.1058-1068.2001.
33. Aviram, N., Thornal, A.N., Zeevi, D., and Marraffini, L.A. (2022). Different modes of spacer acquisition by the Staphylococcus epidermidis type III-A CRISPR-Cas system. Nucleic Acids Res. *50*, 1661–1672. https://doi.org/10.1093/nar/gkab1299.

34. Vialetto, E., Yu, Y., Collins, S.P., Wandera, K.G., Barquist, L., and Beisel, C.L. (2022). A target expression threshold dictates invader defense and prevents autoimmunity by CRISPR-Cas13. Cell Host Microbe *30*, 1151–1162.e6. https://doi.org/10.1016/j.chom.2022.05.013.

35. Heler, R., Samai, P., Modell, J.W., Weiner, C., Goldberg, G.W., Bikard, D., and Marraffini, L.A. (2015). Cas9 specifies functional viral targets during CRISPR-Cas adaptation. Nature *519*, 199–202. https://doi.org/10.1038/nature14245.

36. McGinn, J., and Marraffini, L.A. (2016). CRISPR-Cas Systems Optimize Their Immune Response by Specifying the Site of Spacer Integration. Mol. Cell *64*, 616–623. https://doi.org/10.1016/j.molcel.2016.08.038.

37. Wright, A.V., and Doudna, J.A. (2016). Protecting genome integrity during CRISPR immune adaptation. Nat. Struct. Mol. Biol. *23*, 876–883. https://doi.org/10.1038/nsmb.3289.

38. Lauer, P., Chow, M.Y.N., Loessner, M.J., Portnoy, D.A., and Calendar, R. (2002). Construction, characterization, and use of two Listeria monocytogenes site-specific phage integration vectors. J. Bacteriol. *184*, 4177–4186. https://doi.org/10.1128/JB.184.15.4177-4186.2002.

39. Grindley, N.D.F., Whiteson, K.L., and Rice, P.A. (2006). Mechanisms of site-specific recombination. Annu. Rev. Biochem. *75*, 567–605. https://doi.org/10.1146/annurev.biochem.73.011303.073908.

40. Vink, J.N.A., Baijens, J.H.L., and Brouns, S.J.J. (2021). PAM-repeat associations and spacer selection preferences in single and co-occurring CRISPR-Cas systems. Genome Biol. *22*, 281. https://doi.org/10.1186/s13059-021-02495-9.

41. Vlot, M., Houkes, J., Lochs, S.J.A., Swarts, D.C., Zheng, P., Kunne, T., Mohanraju, P., Anders, C., Jinek, M., van der Oost, J., et al. (2018). Bacteriophage DNA glucosylation impairs target DNA binding by type I and II but not by type V CRISPR-Cas effector complexes. Nucleic Acids Res. *46*, 873–885. https://doi.org/10.1093/nar/gkx1264.

42. Silas, S., Lucas-Elio, P., Jackson, S.A., Aroca-Crevillén, A., Hansen, L.L., Fineran, P.C., Fire, A.Z., and Sánchez-Amat, A. (2017). Type III CRISPR-Cas systems can provide redundancy to counteract viral escape from type I systems. eLife *6*, e27601. https://doi.org/10.7554/eLife.27601.

43. Williams, M.C., Reker, A.E., Margolis, S.R., Liao, J., Wiedmann, M., Rojas, E.R., and Meeske, A.J. (2023). Restriction endonuclease cleavage of phage DNA enables resuscitation from Cas13-induced bacterial dormancy. Nat. Microbiol. *8*, 400–409. https://doi.org/10.1038/s41564-022-01318-2.

44. Camargo, A.P., Nayfach, S., Chen, I.-M.A., Palaniappan, K., Ratner, A., Chu, K., Ritter, S.J., Reddy, T.B.K., Mukherjee, S., Schulz, F., et al. (2022). IMG/VR v4: an expanded database of uncultivated virus genomes within a framework of extensive functional, taxonomic, and ecological metadata. Nucleic Acids Res. *51*, D733–D743. https://doi.org/10.1093/nar/gkac1037.

45. Camargo, A.P., Call, L., Roux, S., Nayfach, S., Huntemann, M., Palaniappan, K., Ratner, A., Chu, K., Mukherjeep, S., Reddy, T.B.K., et al. (2024). IMG/PR: a database of plasmids from genomes and metagenomes with rich annotations and metadata. Nucleic Acids Res. *52*, D164–D173. https://doi.org/10.1093/nar/gkad964.

46. Camarillo-Guerrero, L.F., Almeida, A., Rangel-Pineros, G., Finn, R.D., and Lawley, T.D. (2021). Massive expansion of human gut bacteriophage diversity. Cell *184*, 1098–1109.e9. https://doi.org/10.1016/j.cell.2021.01.029.

47. Nayfach, S., Páez-Espino, D., Call, L., Low, S.J., Sberro, H., Ivanova, N.N., Proal, A.D., Fischbach, M.A., Bhatt, A.S., Hugenholtz, P., et al. (2021). Metagenomic compendium of 189,680 DNA viruses from the human gut microbiome. Nat. Microbiol. *6*, 960–970. https://doi.org/10.1038/s41564-021-00928-6.

48. Langmead, B., and Salzberg, S.L. (2012). Fast gapped-read alignment with Bowtie 2. Nat. Methods *9*, 357–359. https://doi.org/10.1038/nmeth.1923.

49. Crooks, G.E., Hon, G., Chandonia, J.M., and Brenner, S.E. (2004). WebLogo: a sequence logo generator. Genome Res. *14*, 1188–1190. https://doi.org/10.1101/gr.849004.

50. Russel, J., Pinilla-Redondo, R., Mayo-Muñoz, D., Shah, S.A., and Sørensen, S.J. (2020). CRISPRCasTyper: Automated Identification, Annotation, and Classification of CRISPR-Cas Loci. CRISPR J. *3*, 462–469. https://doi.org/10.1089/crispr.2020.0059.

51. Rice, P., Longden, I., and Bleasby, A. (2000). EMBOSS: the European Molecular Biology Open Software Suite. Trends Genet. *16*, 276–277. https://doi.org/10.1016/s0168-9525(00)02024-2.

52. Ciciani, M., Demozzi, M., Pedrazzoli, E., Visentin, E., Pezzè, L., Signorini, L. F., Blanco-Miguez, A., Zolfo, M., Asnicar, F., Casini, A., et al. (2022). Automated identification of sequence-tailored Cas9 proteins using massive metagenomic data. Nat. Commun. *13*, 6474. https://doi.org/10.1038/s41467-022-34213-9.

53. Meeske, A.J., and Marraffini, L.A. (2018). RNA Guide Complementarity Prevents Self-Targeting in Type VI CRISPR Systems. Mol. Cell *71*, 791–801.e3. https://doi.org/10.1016/j.molcel.2018.07.013.

Please cite this article in press as: Margolis and Meeske, Crosstalk between three CRISPR-Cas types enables primed type VI-A adaptation in *Listeria seeligeri*, Cell Host & Microbe (2025), https://doi.org/10.1093/nar/gkx1264

STAR★METHODS

KEY RESOURCES TABLE

REAGENT or RESOURCE	SOURCE	IDENTIFIER
Bacterial and virus strains		
All bacterial strains and phages used in this study are listed in Table S2	This paper	N/A
Chemicals, peptides, and recombinant proteins		
Chloramphenicol	VWR	CAS: 56-75-7; Cat# 97061-244
Kanamycin Monosulfate	GoldBio	CAS: 25389-94-0; Cat# K-120-5
Ampicillin Sodium Salt	VWR	CAS: 69-52-3; Cat# 97061-442
Erythromycin	Sigma	CAS: 114-07–8; Cat# E5389
Oxacillin sodium salt	VWR	CAS: 1173-88-2; Cat# 103466-954
Nalidixic acid sodium salt	VWR	CAS: 3374-05–8; Cat# AAJ63550-14
Anhydrotetracycline hydrochloride	VWR	CAS: 13803-65-1; Cat# AAJ66688-MB
Lysozyme	VWR	CAS: 12650-88-3; Cat# AAJ60701-06
N-lauroylsarcosine	VWR	CAS: 137-16-6; Cat# 97062-270
Phenol: chloroform: iso-amyl alcohol (25:24:1)	VWR	CAS: 136112-00-0; Cat# 97064-694
Q5 High-Fidelity DNA polymerase	NEB	Cat# M0491L
5-bromo-4-chloro-3-indolyl β-d-galactopyranoside	GoldBio	CAS: 7240-90-6; Cat# X4281C10
Isopropyl-β-D-thiogalactopyranoside	GoldBio	CAS: 367-93-1; Cat# I2481C25
Imidazole	VWR	CAS: 288-32-4; Cat# 97065-016
Phenylmethylsulfonyl fluoride	Thermo Scientific	CAS: 329-98-6; Cat# 36978
DNAseI	GoldBio	CAS: 9003-98-9; Cat# D-303-100
Ni-NTA agarose resin	Millipore Sigma	Cat# 70666-4
Ulp1-His protease	Gift from Monica Guo	N/A
Q5 Hot Start High-Fidelity 2x Master Mix	NEB	Cat# M0494L
Mitomycin C	VWR	CAS: 50-07-7; Cat# 22694-0020
T4 DNA Ligase	NEB	Cat# M0202L
T5 exonuclease	NEB	Cat# M0663L
Taq DNA ligase	NEB	Cat# M0208L
Critical commercial assays		
QIAquick Gel Extraction Kit	QIAGEN	Cat# 28704
TrueSeq Nano DNA Library Prep	Illumina	Cat# 20015964
DNA Clean & Concentrator-5 kit	Zymo Research	Cat# D4004
QIAprep Spin Miniprep Kit	QIAGEN	Cat# 27104
Deposited data		
Raw sequencing data	This paper	SRA: PRJNA1246610
IMG/VR v4	Camargo et al.[44]	https://genome.jgi.doe.gov/portal/IMG_VR
IMG/PR	Camargo et al.[45]	https://genome.jgi.doe.gov/portal/IMG_PR/IMG_PR.home.html
GPD	Camarillo-Guerrero et al.[46]	https://ftp.ebi.ac.uk/pub/databases/metagenomics/genome_sets/gut_phage_database/
MGV	Nayfach et al.[47]	https://portal.nersc.gov/MGV
Oligonucleotides		
All oligonucleotides used in this study are listed in Table S2.	This paper	N/A

(*Continued on next page*)

Continued

REAGENT or RESOURCE	SOURCE	IDENTIFIER
Recombinant DNA		
All plasmids and synthetic genes used in this study are listed in Table S2.	This paper	N/A
Software and algorithms		
Prism v10.4.1	Graphpad	https://www.graphpad.com/
Adobe Illustrator v26.0.2	Adobe	https://www.adobe.com/products/illustrator.html
R v4.3.1	R Foundation	https://www.r-project.org/
Python v3.9.7	Python Software Foundation	https://www.python.org/downloads/
GNU bash v3.2.57	Free Software Foundation	https://ftp.gnu.org/gnu/bash/
Bowtie2	Langmead and Salzberg[48]	http://bowtie-bio.sourceforge.net/bowtie2/index.shtml
Weblogo	Crooks et. al.[49]	https://weblogo.threeplusone.com/
CRISPRCasTyper	Russel et. al.[50]	https://github.com/Russel88/CRISPRCasTyper
EMBOSS	Rice et. al.[51]	https://emboss.sourceforge.net/
PAMpredict	Ciciani et. al.[52]	https://github.com/Matteo-Ciciani/PAMpredict
Other		
NextSeq or NovaSeq X Plus	Illumina	N/A
Superdex 75 Increase 10/300 GL	Cytiva	Cat# 29148721

EXPERIMENTAL MODEL DETAILS

Bacterial strains and growth conditions

All bacterial strains used in this study are noted in Table S2. *Listeria seeligeri* strains were cultured in Brain Heart Infusion (BHI) broth or agar at 30 °C, and *Escherichia coli* strains were grown in lysogeny broth (LB) or agar at 37°C. Appropriate antibiotics were supplemented at the following concentrations: 50 μg/ml kanamycin, 100 μg/ml ampicillin, 1 μg/ml erythromycin, 25 μg/ml chloramphenicol for *E. coli*, 10 μg/ml chloramphenicol for *L. seeligeri*, 8 μg/ml oxacillin, 50 μg/ml nalidixic acid. Liquid cultures were inoculated from single colonies and grown with shaking. Most plasmids were initially cloned in Turbo Competent *E. coli* (New England Biolabs) and miniprepped, except plasmids for the in vitro assays, which were cloned in DH5α. For introduction into *L. seeligeri*, plasmids were transformed into one of the following conjugative donor strain of *E. coli*: β2163 Δ*dapA* for allelic exchange, or S-17 λpir or SM10 λpir for all other plasmid introduction.

Phage propagation

Phage stocks were generated from single plaques formed on top agar lawns of LS1 ΔRM1 ΔRM2 $\Delta CRISPR_{VI\text{-}A}$. Top agar lawns were made by combining 100 μL of overnight culture with $CaCl_2$ and 5 mL of molten BHI agar. In the case of $U153_{lyt}$, cells also contained pAM324, which expresses Cas9 targeting the phage integrase, allowing for isolation of a spontaneous phage mutant that lost the entire lysogenic operon (confirmed by PCR with oSM101 and oSM288). Phage stocks were made by infecting 5 mL of *L. seeligeri* at OD_{600} of 0.1 with the plaque, allowing infection to proceed overnight, and filtering the resulting lysate through a 0.45-μm-pore syringe filter. Phage stocks were stored at 4°C.

METHOD DETAILS

Plasmid construction

Details of plasmid construction, along with all plasmids and oligonucleotides used in this study can be found in Table S2. For spacer cloning, oligos were annealed in T4 ligase buffer, starting at 95°C and slowly cooling to room temperature. Annealed oligos were then combined with restriction-digested plasmid and T4 DNA ligase for 30 minutes at room temperature before transforming into Turbo competent *E. coli*. All other plasmids were constructed by Gibson assembly. Inserts were amplified by PCR, gel purified, and incubated with restriction digested plasmids in Gibson master mix (containing T5 exonuclease, Q5 DNA polymerase, and Taq ligase) for 30 minutes at 50°C before transforming into competent *E. coli*. Pure plasmids were isolated using QIAprep Spin Miniprep Kit per the manufacturer's protocol.

E. coli–L. seeligeri conjugation

Donor *E. coli* strains S-17 λpir, SM10 λpir, or β2163 Δ*dapA* (for allelic exchange) carrying *E. coli–Listeria* shuttle vectors were cultured overnight in LB medium with the appropriate antibiotic: 25 μg/ml chloramphenicol (for pPL2e-derived plasmids), 50 μg/ml kanamycin (for pAM326-derived plasmids), or 100 μg/ml ampicillin (for pAM8-derived plasmids). Recipient *L. seeligeri* strains were grown

overnight in BHI medium supplemented with 1 μg/ml erythromycin (for pPL2e-derived plasmids), 10 μg/ml chloramphenicol (for marked lysogens or pAM8-derived plasmids), or 50 μg/ml kanamycin (for pAM326-derived plasmids) at 30°C. The saturated donor and recipient cultures (100 μl each) were combined in 10 ml BHI and concentrated onto a 0.45-μm membrane filter disc (Millipore-Sigma) using vacuum filtration. The filter was then placed on BHI agar containing 8 μg/ml oxacillin, which weakens the cell wall, enhancing conjugation, and incubated at 37°C for 4 hours. After incubation, the cells were resuspended in 2 ml BHI and plated on selective BHI medium containing 50 μg/ml nalidixic acid, which kills donor E. coli but not recipient Listeria, along with the appropriate antibiotic for plasmid selection. Transconjugants were isolated after 2–3 days of incubation at 30°C.

Cas1-2 induction experiments

L. seeligeri strains were grown overnight in BHI with the appropriate antibiotics. The next day, cultures were diluted 1:1000 into BHI with antibiotics and 100 ng/mL anhydrotetracycline (aTc) for induction of the Ptet promoter. After 24 hours, cultures were similarly passaged once more into fresh media with aTc and after another 24 hours (48 hours total induction) cells were pelleted by centrifugation and frozen at -20°C prior to genomic DNA (gDNA) extraction.

Sample preparation and array amplification for next-generation sequencing

Cell pellets were resuspended in PBS and lysed by incubation with 2mg/mL lysozyme and 1% N-lauroylsarcosine. Genomic DNA was isolated by phenol/chloroform extraction followed by ethanol precipitation. 100ng of genomic DNA were used as input for the type VI-A array enrichment PCR with Q5 High-Fidelity DNA polymerase (NEB) and 0.4μM final concentration of each primer: oDB026 (binds to preexisting leader-adjacent spacer (spc1)), and oSM039, oSM040, oSM041 (each of which binds to the type VI-A repeat with the final two 3' nucleotides differing to match any nucleotide except those of spc1). Reactions were performed with a 57.5°C primer annealing temperature and 10 second extension time, and then run on a 2% agarose gel from which bands larger than 100bp were extracted using a QIAquick Gel Extraction Kit. Amplicons were prepared for sequencing with the TrueSeq Nano DNA Library Prep protocol (Illumina) and sequenced with the NextSeq or NovaSeq X Plus platforms (Illumina). Raw sequencing reads are available through SRA Accession: PRJNA1246610.

Gene deletions

Allelic replacement in *L. seeligeri* was performed as previously described.[53] Briefly, 500-1000 bp homologous sequences flanking the region targeted for replacement were cloned into the suicide plasmid pAM215, which contains lacZ and chloramphenicol resistance (cat) markers. The plasmid was introduced into *L. seeligeri* strains via conjugation as outlined above, and 100 μl of the resuspended cells was plated on selective media containing 50 μg/ml nalidixic acid and 15 μg/ml chloramphenicol. Transconjugants (integrants) were isolated and passaged (grown to saturation, then diluted 1,000-fold) 3 times in BHI without antibiotics. The passaged cultures were then diluted and plated on BHI plates with 100 μg/ml 5-bromo-4-chloro-3-indolyl β-d-galactopyranoside (X-gal), followed by incubation for 2–3 days at 30°C. White (lacZ–) colonies (excisants) were selected, confirmed to be chloramphenicol-sensitive, and the deletion was verified by PCR with primers flanking the target region.

Cas1 and Cas2 purification

Codon optimized *L. seeligeri* type II-C Cas1 and Cas2 were cloned into pKS22b-His-SUMO, and the resulting plasmids were separately transformed into BL21(DE3) *E. coli*. Cells were grown in 1 L of LB with 100 μg/ml carbenicillin shaking at 37°C until reaching an OD_{600} of 0.6, and then induced overnight at 18°C with 1 mM isopropyl-β-D-thiogalactopyranoside (IPTG). The cells were pelleted, resuspended in lysis buffer (50 mM Tris-HCl, pH 7.5, 500 mM NaCl, 20 mM imidazole, 10% glycerol, 1mM DTT, 1mg/ml lysozyme, 1mM PMSF, 15 units DNAseI, 0.5mM MgCl2), and incubated on ice for one hour before sonication. Sonicated lysates were centrifuged, and the cleared lysates were passed over Ni-NTA agarose resin (MilliporeSigma) at 4°C.The resin was washed with wash buffer (50 mM Tris-HCl, pH 7.5, 500 mM NaCl, 20 mM imidazole, 10% glycerol, 1mM DTT) and the protein eluted in wash buffer supplemented with 400 mM imidazole. Eluted protein was dialyzed overnight in fresh wash buffer with Ulp1-His protease to remove the His-SUMO tag. The next day, the protein was again passed over Ni-NTA resin to remove both the protease and any remaining uncleaved protein. The flowthrough was collected, concentrated, and further purified on a Superdex -75 Increase 10/300 in protein buffer (50 mM Tris-HCl, pH 7.5, 500 mM NaCl, 10% glycerol, 1mM DTT). Fractions containing the protein of interest were combined, concentrated, aliquoted, and stored at -80°C.

In vitro integration assays

Oligos oSM97/oSM98[37] were hybridized in integration buffer (20mM Tris-HCl pH 8, 25 mM NaCl, 10 mM $MgCl_2$, 1mM DTT, 10% DMSO) by heating to 95°C and slowly cooling to room temperature to create a 30bp protospacer with 4bp overhangs. 5 μM Cas1 and Cas2 were combined and incubated on ice for 30 minutes, then diluted to 47 nM and incubated with 200 nM protospacer on ice for 15 minutes. 20 nM of target plasmids that had been purified from DH5α *E. coli* were then added and incubated at 37°C for 30 minutes, then quenched with 0.4% SDS and 50 mM EDTA. Plasmids were purified using the DNA Clean & Concentrator-5 kit (Zymo), eluted in 8 μl of water, and 1 μl of 1:6 diluted plasmid was used as input for half-site integration PCRs. PCRs were performed using Q5 Hot Start High-Fidelity 2x Master Mix (NEB) per the manufacturer's instructions with a 30 second extension time using

primers oSM097 (p1 in Figure 3) and oSM029 (p2 in Figure 3). Reaction products were analyzed on a 1.5% agarose gel containing ethidium bromide. PCR products were sequenced to confirm that bands corresponded to the expected leader-adjacent half-site integration.

Phage infections

All phage infections were performed in BHI with 5 mM $CaCl_2$. Top agar lawns were made by combining 100 μL of overnight culture with $CaCl_2$ and 5 mL of molten BHI agar. Phage stock was titered on top agar lawns to identify the plaque forming units (PFU) per μL, and this information was used to infect experimental strains at a multiplicity of infection of 0.1. Infection and addition of atc to induce Cas1-2 occurred at the same time. After 48 hours of infection, cells were pelleted by centrifugation and stored at -20°C prior to gDNA extraction. To determine PFU production by lysogens, cultures at OD_{600} of 0.1 were treated with 2 μg/mL mitomycin C overnight, filtered and titered as above.

U153-cmR construction

A constitutively expressed *cat* gene was inserted into a non-essential region of the U153 genome, downstream of the lysin gene. Briefly, the kanR plasmid pAM591 was constructed containing the *cat* gene flanked by 500 bp of U153 genomic sequence surrounding the desired insertion site. After introducing pAM591 into LS1 via conjugation, the resultant strain was infected with phage U153 to enable recombination with pAM591. Infection was performed at an MOI of 0.1, proceeded overnight, and a phage stock was harvested as above. This stock represented a heterogeneous mixture of wild-type and recombinant phage, which was then used to infect a fresh LS1 culture at an MOI of 1 for 1 hour. Lysogens were then selected by plating the infected cells on BHI + chloramphenicol. Chloramphenicol-resistant lysogens were confirmed to be kanamycin-sensitive, then the recombinant prophage was induced by treatment with 2 μg/mL mitomycin C, and plaques were isolated on a lawn of wild-type LS1 infected with the induced culture filtrate. A stock of recombinant U153-cmR was prepared by expanding a single plaque as above.

Bioinformatic analysis of CRISPR loci

CRISPRCasTyper[50] with default settings was used to analyze CRISPR-Cas loci in all 2712 *Listeria spp.* genomes available from NCBI. The resultant cas_operons.tab output files were parsed to tabulate the number of Type I-B, II-A, II-C, and VI-A loci, and occurrence of associated Cas1 and Cas2 alleles. Type II-A and II-C loci were distinguished by Csn2 family designation. For bioinformatic analysis of CRISPR loci beyond *Listeria spp.*, we first collected 1089 genomes encoding proteins with similarity (BLASTp E-value 1E-4) to diverse representatives of Cas13a, Cas13b1, Cas13b2, Cas13c, and Cas13d protein families. As above, CRISPRCasTyper was used to annotate CRISPR-Cas loci in each genome. Repeat sequences were extracted and aligned using the needle program in the EMBOSS toolkit.[51] Spacer targets were identified using PAMpredict[52] searching the IMG/VR,[44] IMG/PR,[45] GPD,[46] and MGV[47] databases with default settings.

Cas9 phylogenetic tree construction

39 diverse type II-A, II-B, and II-C Cas9 protein sequences were aligned with MAFFT using default settings. The resulting alignment was used to generate a statistically-supported phylogenetic tree using the neighbor-joining method in MEGAv11 with default settings and 1000 bootstrap replications.

QUANTIFICATION AND STATISTICAL ANALYSIS

Statistical tests, significance, and number of biological replicates (n) can be found in the figure legends. Two-tailed Student's t tests were used in Figures 1D and 2C. Spearman's rank correlation test was used in Figures S2D–S2F. Statistical tests were performed in Graphpad Prism or R.

High throughput sequencing data analysis

Newly acquired spacer sequences, defined as those flanked by spc1 and direct repeat on one side, and a second repeat on the other side, were extracted from the raw Illumina FASTQ files. Instances of each spacer sequence were counted and unique spacers were mapped to host, plasmid, or phage genomes using Bowtie2[48] with default parameters. Sequences mapping to the existing type VI-A array were assumed to be PCR artifacts and discarded (for samples with few acquired spacers, these were the majority of reads). Next, unique mapped spacers with over 10 instances were tallied for defined bins in each genome. All spacers derived from the same strand and alignment coordinates were considered to be the same unique spacer. All plots were made in R, and replicates were combined for plotting as indicated in the figure legends. Plots with full counts of all newly acquired spacers mapped to the genome for each replicate can be found in supplemental figures. For determining mRNA targeting ability of newly acquired spacers, spacers were compared to the strand and orientation of LS1 open reading frames using a Python script adapted from Hoikkala et al.[22] To test for correlation with transcription, spacer abundance per bin was compared to transcription levels of previously published RNA-seq data[25] using a Spearman's rank correlation test. To generate sequence motifs, the 30 bp regions flanking all 30 bp spacer sequences that mapped to the LS1 genome were extracted and analyzed using WebLogo.[49]